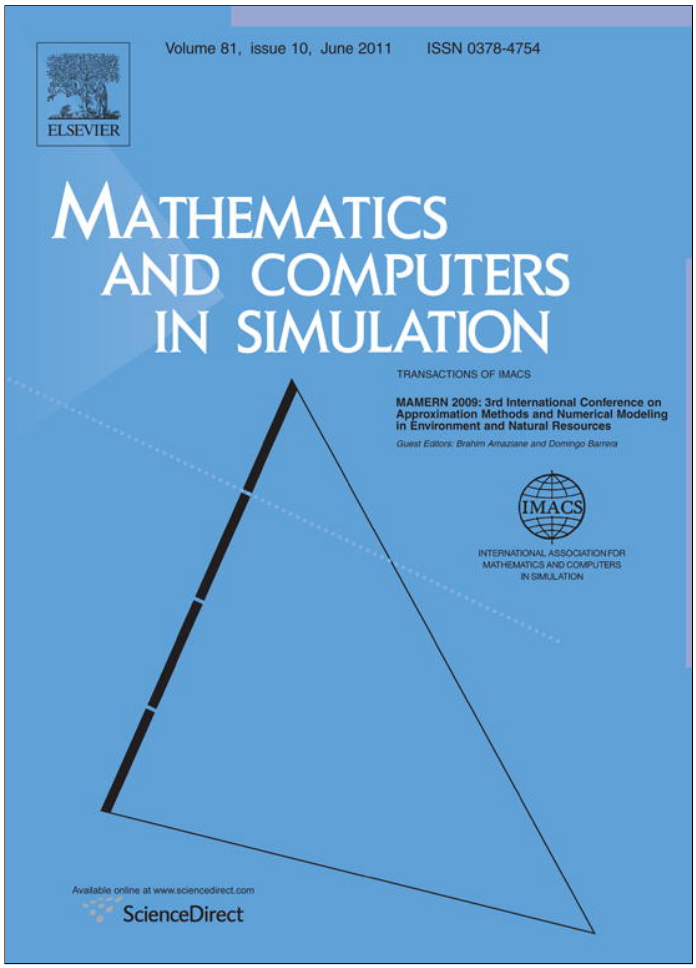

Available online at www.sciencedirect.com
ScienceDirect
Mathematics and Computers in Simulation 81 (2011) 1949–1961
MATHEMATICS AND COMPUTERS IN SIMULATION
www.elsevier.com/locate/matcom

On optimal convergence rate of finite element solutions of boundary value problems on adaptive anisotropic meshes

Abdellatif Agouzal [a], Konstantin Lipnikov [b], Yuri V. Vassilevski [c,*]

[a] *U.M.R. 5585 – Equipe d'Analyse Numerique Lyon Saint-Etienne Universite de Lyon 1, Laboratoire d'Analyse Numerique Bat. 101, 69 622 Villeurbanne Cedex, France*
[b] *Los Alamos National Laboratory Los Alamos, NM 87545, USA*
[c] *Institute of Numerical Mathematics, Russian Academy of Sciences, Moscow 119333, Russia*

Received 16 November 2009; received in revised form 15 July 2010; accepted 8 December 2010
Available online 30 December 2010

Abstract

We describe a new method for generating meshes that minimize the gradient of a discretization error. The key element of this method is construction of a tensor metric from edge-based error estimates. In our papers [1–4] we applied this metric for generating meshes that minimize the gradient of P_1-interpolation error and proved that for a mesh with N triangles, the L^2-norm of gradient of the interpolation error is proportional to $N^{-1/2}$. In the present paper we recover the tensor metric using hierarchical a posteriori error estimates. Optimal reduction of the discretization error on a sequence of adaptive meshes will be illustrated numerically for boundary value problems ranging from a linear isotropic diffusion equation to a nonlinear transonic potential equation.

Keywords: Metric-based adaptation; Finite element method; Quasi-optimal meshes

1. Introduction

Generation of adaptive meshes is the active research area. The paper is devoted to generation of meshes which minimize the energy norm of finite element solutions to boundary value problems. The minimum is sought over the set of conformal triangulations with a fixed number of simplexes. An approximate solution of the minimization problem is deemed sufficient if (a) the discretization error is close to that on the optimal mesh and (b) the error reduction rate on a sequence of generated meshes is optimal. We call such meshes *quasi-optimal*.

In [1–4], we analyzed the problem of minimizing the L^p-norm of the gradient of the interpolation error and proposed a numerical method for generation of d-dimensional quasi-optimal meshes. The method recovers a tensor metric inside each simplex from function values at the simplex vertices and edge midpoints. The analysis is based on a geometric representation of the error and a relaxed saturation assumption. In [1] we applied the method to finite element discretizations of linear elliptic PDEs. The numerical experiments have shown optimal reduction of hierarchical error estimates on anisotropic meshes. In this paper, we analyze numerically robustness

* Corresponding author.
E-mail addresses: agouzal@univ-lyon1.fr (A. Agouzal), lipnikov@lanl.gov (K. Lipnikov), vasilevs@dodo.inm.ras.ru (Y.V. Vassilevski).

0378-4754/$36.00 © 2010 IMACS. Published by Elsevier B.V. All rights reserved.
doi:10.1016/j.matcom.2010.12.027

of hierarchical error estimates for boundary value problems with anisotropic solutions. The selected set of problems includes diffusion, convection-diffusion, the Stokes and Navier–Stokes equations. We present numerical results which demonstrate quasi-optimality of two-dimensional anisotropic meshes for finite element solution of these problems.

The existing theoretical results [1,2,13,17,18,23] indicate that a posteriori error estimates may and should be efficient and reliable on anisotropic meshes aligned with the solution. However, the theory makes a few assumptions that are difficult to verify *a priori*, such as the saturation assumption on anisotropic meshes. Also, there are *no* theoretical results showing convergence of adaptive iterations, especially in case where the initial mesh is not aligned with the solution. Thus, numerical analysis remains so far the only tool available to us.

In our method, no assumption of shape regularity is imposed on quasi-optimal and optimal meshes. The shape of simplexes is controlled by a specially designed metric $\mathfrak{M}$ which is recovered from *a posteriori* error estimates prescribed to mesh edges. The volume and the perimeter of a d-simplex measured in this metric bound the error norm from the above and below. To build a quasi-optimal mesh, we use the error equidistribution principle that suggests to balance $\mathfrak{M}$-volumes and $\mathfrak{M}$-perimeters to produce a mesh that is quasi-uniform in metric $\mathfrak{M}$ [21,22]. The mesh generation algorithm employs a sequence of local mesh modifications [9,21]; therefore, it is easy to parallelize [10,19]. These modifications include vertex addition, deletion and relocation, and edge/face swapping.

Another approach to derivation of an optimal tensor metric uses the Hessian of a discrete solution [7,8,11,15,16,21]. For a piecewise linear finite element solution, its Hessian can be defined only in a weak sense. The lack of strong convergence of the discrete Hessian to the continuous one during mesh refinement is one of the problems in analysis of the Hessian-based methods. Comparison of the two methodologies for metric generation is beyond the scope of this paper.

For the sake of simplicity, we restrict our presentation to conformal triangulations on a plane, although all the results can be extended to d-dimensional simplicial meshes.

The paper outline is as follows. In Section 2, we derive a local metric from edge-based error estimates. In Section 3, we derive estimates for the global error. In Section 4, we illustrate with numerical experiments optimal reduction rate of the interpolation error. In Section 5, we describe a hierarchical error estimator. In Section 6, we analyze numerically robustness of this estimator for minimization of the discretization error.

2. Local interpolation error estimates and metric recovery

In this section, we use an interpolation problem as the preliminary step for the subsequent analysis of a discretization error. We highlight three basic points of our method. First, the error in a triangle can be represented as a sum of errors on its edges. Second, this representation is not unique. Third, the edge-based errors define the tensor metric which controls the error norm.

Let Ω be a bounded polygonal domain and Ω_h be its conformal triangulation with N_h triangles. The area of a triangle Δ and its perimeter in a metric $\mathfrak{M}$ are denoted by $|\Delta|_{\mathfrak{M}}$ and $|\partial\Delta|_{\mathfrak{M}}$, respectively. Let $\mathcal{I}_1 u$ be the continuous piecewise linear Lagrange interpolant of u, and $\mathcal{I}_{1,\Delta} u$ be its restriction to Δ. Our goal is to generate meshes that minimize the L^2-norm of the gradient of the interpolation error $e = u - \mathcal{I}_1 u$.

Let us consider a triangle Δ with vertices $\mathbf{v}_i$, $i = 1, 2, 3$, edge vectors $\mathbf{e}_k = \mathbf{v}_i - \mathbf{v}_j$, $1 \le i < j \le 3$, and mid-edge points $\mathbf{c}_k$, $k = 1, 2, 3$. Let λ_i, $i = 1, 2, 3$, be the linear functions on Δ such that $\lambda_i(\mathbf{v}_j) = \delta_{ij}$, where δ_{ij} is the Kronecker symbol. For every edge $\mathbf{e}_k$, we define the quadratic bubble function $b_k = \lambda_i \lambda_j$.

To simplify error analysis, we employ the divide and conquer approach. Most of the analysis is done for quadratic functions. Then, the obtained results are extended to general functions. Let u be a general continuous function. On each simplex Δ, we consider its quadratic approximation $u_2 = \mathcal{I}_{2,\Delta} u$, where $\mathcal{I}_{2,\Delta} u$ is the Lagrange interpolant of u. The interpolation error for u_2 is

$$e_2 = u_2 - \mathcal{I}_{1,\Delta} u_2 = 4 \sum_{k=1}^{3} (u_2(\mathbf{c}_k) - \mathcal{I}_{1,\Delta} u_2(\mathbf{c}_k))\, b_k \equiv \sum_{k=1}^{3} \gamma_k\, b_k. \tag{1}$$

Note that calculation of γ_k requires to evaluate u_2 at three points on edge $\mathbf{e}_k$, two end-points and one mid-point. The L^2-norm of gradient of e_2 is given by

$$\|\nabla e_2\|^2_{L^2(\Delta)} = \left\| \sum_{k=1}^{3} \gamma_k \nabla b_k \right\|^2_{L^2(\Delta)} = |\Delta| (\mathbb{B}\,\boldsymbol{\gamma},\ \boldsymbol{\gamma}),$$

where $\boldsymbol{\gamma}$ is the vector with 3 components γ_k and $\mathbb{B}$ is the 3×3 symmetric positive definite matrix with entries $\mathbb{B}_{k,l} = |\Delta|^{-1} \int_\Delta \nabla b_k \cdot \nabla b_l \, \mathrm{d}V$. This error is only a number; therefore, it does not provide any directional information. To recover this information, we split this error into 3 edge-based error estimates $\alpha_k \geq 0$ such that

$$\|\nabla e_2\|^2_{L^2(\Delta)} = |\Delta| \sum_{k=1}^{3} \alpha_k \qquad \text{and} \qquad \sum_{k=1}^{3} \alpha_k = (\mathbb{B}\boldsymbol{\gamma}, \boldsymbol{\gamma}). \tag{2}$$

Generally speaking, there exists a freedom in the choice of α_k. We are going to exploit the detailed structure of the error. Looking back at formula (1), we observe that

$$\|e_2\|_{L^\infty(\mathbf{e}_k)} = \frac{1}{4} |\gamma_k|.$$

This estimate does not depend on the shape of Δ and is the same for two triangles that share edge $\mathbf{e}_k$. We propose to select $\alpha_k = c_\Delta \, |\gamma_k|$, where the factor c_Δ is the same for all edges in the simplex. The simple calculations give

$$\alpha_k = |\gamma_k| \, (\mathbb{B}\boldsymbol{\gamma},\ \boldsymbol{\gamma}) \left(\sum_{k=1}^{3} |\gamma_k| \right)^{-1}. \tag{3}$$

A similar selection will be made in analysis of the discretization error. The next lemma shows existence of a tensor metric that controls the sum of α_k.

Lemma 1. *Let α_k, $k = 1, 2, 3$, be the values prescribed to edges of a triangle Δ such that $\alpha_k \geq 0$ and $\alpha_1 + \alpha_2 + \alpha_3 > 0$. Then, there exists a constant tensor metric $\widetilde{\mathfrak{M}}_\Delta$ such that*

$$\frac{1}{\sqrt{2}} |\Delta|_{\widetilde{\mathfrak{M}}_\Delta} \leq \sum_{k=1}^{3} \alpha_k \leq |\partial\Delta|^2_{\widetilde{\mathfrak{M}}_\Delta}. \tag{4}$$

The proof is sketched below and the detailed proof can be found in [2,4]. Let us consider the quadratic function $v_2 = -\frac{1}{2} \sum_{k=1}^{3} \alpha_k b_k$ and denote its Hessian by $\mathbb{H}(v_2)$. If $\det(\mathbb{H}(v_2)) \neq 0$, we set $\widetilde{\mathfrak{M}}_\Delta = |\mathbb{H}(v_2)|$ where $|\mathbb{H}(v_2)|$ is the spectral module of $\mathbb{H}(v_2)$. Otherwise, we increase slightly the largest α_k so that the modified function v_2 has a non-singular Hessian. In practice, increase by 1% was sufficient for all numerical experiments.

The derivation of metric $\widetilde{\mathfrak{M}}_\Delta$ suggests a simple motivation for our choice of α_k. Let $\mathbb{H}(v_2)$ be definite. Since the bubble function b_k is non-zero only on one edge, we get

$$(\widetilde{\mathfrak{M}}_\Delta \mathbf{e}_k, \mathbf{e}_k) = \frac{1}{2} \alpha_k (|\mathbb{H}(b_k)| \mathbf{e}_k, \mathbf{e}_k) = c_\Delta \, |\gamma_k| = 4 \, c_\Delta \, \|e_2\|_{L^\infty(\mathbf{e}_k)}.$$

Recall that c_Δ is the same for all edges of Δ. Thus, when Δ is the $\widetilde{\mathfrak{M}}_\Delta$-equilateral triangle, we get immediately that

$$\|e_2\|_{L^\infty(\mathbf{e}_1)} = \|e_2\|_{L^\infty(\mathbf{e}_2)} = \|e_2\|_{L^\infty(\mathbf{e}_3)}.$$

Thus, the choice (3) means that in a mesh consisting of equal $\widetilde{\mathfrak{M}}_\Delta$-equilateral triangles, we equidistribute the L^2-norm of gradient of error over triangles and the L^∞-norm of error over edges.

Combining (2) and (4), we get the geometric representation of L^2-norm of ∇e_2:

$$\frac{1}{\sqrt{2}} |\Delta| \, |\Delta|_{\widetilde{\mathfrak{M}}_\Delta} \leq \|\nabla e_2\|^2_{L^2(\Delta)} \leq |\Delta| \, |\partial\Delta|^2_{\widetilde{\mathfrak{M}}_\Delta}. \tag{5}$$

In other words, the L^2-norm of the gradient of error is controlled from above by $\widetilde{\mathfrak{M}}_\Delta$-perimeter and from below by $\widetilde{\mathfrak{M}}_\Delta$-area of triangle Δ. The final step is to modify the metric so that the controlling quantities will be measured in the same metric. This is achieved by a simple metric rescaling [2,4]:

$$\mathfrak{M}_\Delta = (\det \widetilde{\mathfrak{M}}_\Delta)^{-1/4}\, \widetilde{\mathfrak{M}}_\Delta \tag{6}$$

for which one has $|\Delta||\Delta|^2_{\widetilde{\mathfrak{M}}_\Delta} = |\Delta|^2_{\mathfrak{M}_\Delta}$ and $|\Delta||\partial\Delta|^2_{\widetilde{\mathfrak{M}}_\Delta} = |\Delta|_{\mathfrak{M}_\Delta}|\partial\Delta|^2_{\mathfrak{M}_\Delta}$.

Lemma 2. *For metric $\mathfrak{M}_\Delta$ defined by (6), it holds*

$$\frac{1}{\sqrt{2}}|\Delta|^2_{\mathfrak{M}_\Delta} \le \|\nabla e_2\|^2_{L^2(\Delta)} \le |\Delta|_{\mathfrak{M}_\Delta}\, |\partial\Delta|^2_{\mathfrak{M}_\Delta}. \tag{7}$$

Lemma 2 provides the geometric representation of the error norm for a quadratic function u_2. It is shown in [2,4] that this error norm is a good approximation to the same norm of the true error $e = u - \mathcal{I}_{1,\Delta}u$. In order to formulate this result, we introduce the space of symmetric 2×2 matrices $\mathcal{F}$ and define the following norm for a vector $\mathbf{e}_k$:

$$|\|\mathbf{e}_k|\|^2_{|\mathbb{H}|} = \max_{\mathbf{x}\in\Delta} (|\mathbb{H}(\mathbf{x})|\mathbf{e}_k, \mathbf{e}_k). \tag{8}$$

Lemma 3. *Let $u \in C^2(\bar{\Delta})$. Then, there exist a positive constant c_o such that*

$$\|\nabla e_2\|_{L^2(\Delta)} - c_o\, \mathrm{osc}\,(\mathbb{H}, \Delta) \le \|\nabla e_\Delta\|_{L^2(\Delta)} \le \|\nabla e_2\|_{L^2(\Delta)} + c_o\, \mathrm{osc}(\mathbb{H}, \Delta), \tag{9}$$

where

$$\mathrm{osc}(\mathbb{H}, \Delta) = \frac{|\partial\Delta|}{|\Delta|} \inf_{\mathbb{F}\in\mathcal{F}} |\|\partial\Delta|\|^2_{|\mathbb{H}-\mathbb{F}|}.$$

The oscillation term is smaller than the error. Its value depends on the triangle and particular features of the function. For instance, if $u \in C^2(\bar{\Delta})$, and Δ is shape regular, one has $\mathrm{osc}(\mathbb{H}, \Delta) \le C|\partial\Delta|\inf_{\mathbb{F}\in\mathcal{F}}|\mathbb{H} - \mathbb{F}|_\infty$.

3. Global error estimate and quasi-optimal meshes

Let $\mathfrak{M}$ be the tensor metric composed of local metrics $\mathfrak{M}_\Delta$ satisfying Lemma 2. Let Ω_h be a triangulation with N_h cells that is quasi-uniform in metric $\mathfrak{M}$. Thus, $|\partial\Delta|^2_{\mathfrak{M}} \simeq |\Delta|_{\mathfrak{M}}$ and

$$N_h^{-1}|\Omega|_{\mathfrak{M}} \simeq |\Delta|_{\mathfrak{M}_\Delta} \simeq |\partial\Delta|^2_{\mathfrak{M}_\Delta} \quad \forall\Delta\in\Omega_h,$$

where $a \simeq b$ means existence of constants c and C independent of mesh such that $c\,a \le b \le C\,a$. On such a mesh, the following error estimate is held

$$\|\nabla e\|_{L^2(\Omega)} = \left(\sum_{\Delta\in\Omega_h} \|\nabla e\|^2_{L^2(\Delta)}\right)^{1/2} \simeq \left(\sum_{\Delta\in\Omega_h} |\Delta|^2_{\mathfrak{M}_\Delta}\right)^{1/2} \simeq |\Omega|_{\mathfrak{M}}\, N_h^{-1/2}. \tag{10}$$

In other words, the sequence of $\mathfrak{M}$-quasi-uniform meshes provides asymptotically optimal rate for reduction of the L^2-norm of the gradient of error.

In order to generate the $\mathfrak{M}$-quasi-uniform mesh, we use Algorithm 1. The algorithm provides faster convergence when the metric is continuous. To define a continuous metric we use a method of shifts. For every node $\mathbf{a}_i$ in Ω_h, we define the superelement σ_i as the union of all triangles sharing $\mathbf{a}_i$. Then, $\mathfrak{M}(\mathbf{a}_i)$ is defined as one of the metrics in σ_i with the largest determinant. This method always chooses the worst metric in the superelement. To generate a $\mathfrak{M}$-quasi-uniform mesh, we use local mesh modifications described in [21] and implemented in package `Ani2D` (sourceforge.net/projects/ani2d).

Algorithm 1. Adaptive mesh generation

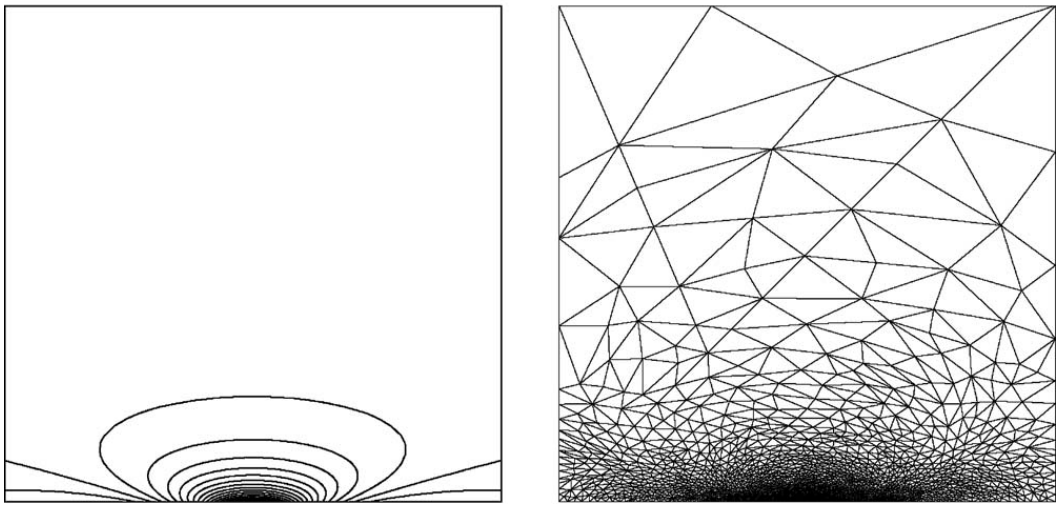

Fig. 1. Isolines of function (11) and the quasi-optimal mesh with roughly 2000 triangles.

1:	Generate an initial mesh Ω_h and compute the metric $\mathfrak{M}$.
2:	**loop**
3:	Generate a new mesh Ω_h that is quasi-uniform in metric $\mathfrak{M}$ and has the prescribed number of triangles.
4:	Recompute the metric $\mathfrak{M}$.
5:	If Ω_h is $\mathfrak{M}$-quasi-uniform, then exit the loop
6:	**end loop**

4. Numerical minimization of the gradient of interpolation error

In the first experiment, we consider the problem of minimizing the L^2-norm of the gradient of the interpolation error for the function from [11]:

$$u(x,\ y) = \frac{(x-0.5)^2 - \left(\sqrt{10}y + 0.2\right)^2}{\left((x-0.5)^2 + \left(\sqrt{10}y + 0.2\right)^2\right)^2}. \tag{11}$$

The computational domain is the unit square $[0,\ 1]^2$. The function has a weak anisotropic singularity at point $(0.5,\ -0.2/\sqrt{10})$ which is outside the computational domain but close to its boundary. Isolines of u are shown on the left picture in Fig. 1.

In the second experiment, we consider the function from [14] with anisotropic features:

$$u(x,\ y) = yx^2 + y^3 + \tanh(6(\sin(5y) - 2x)). \tag{12}$$

The computational domain is the square $[-1,\ 1]^2$. The function is anisotropic along the zigzag curve and changes sharply in the direction normal to this curve (see the left picture in Fig. 3). Table 1 shows the interpolation error

Table 1
The L^2-norm of the gradient of the interpolation error for functions (11) and (12).

$N_h \setminus u$	Function (11)	Function (12)
600	3.9	2.0
2500	1.9	0.88
10,000	1.0	0.44
40,000	0.51	0.22
Rate	0.49	0.53

$\|\nabla(u - \mathcal{I}_{1,\Delta}u)\|_{L^2(\Omega)}$ for both functions. The optimal half-order convergence rate predicted in (10) is clearly observed in both cases.

Triangles in the quasi-optimal meshes have smaller size in regions where the isolines are dense and are stretched along the main direction of the anisotropy.

5. Hierarchical error estimates for finite element solutions of PDEs

In the construction of metric $\mathfrak{M}_\Delta$, the coefficients γ_k of error representation (1) play the important role. In the finite element community, the bubble finite element functions are often used in derivation of error estimates. We suggest to use the coefficients in front of these bubbles to build the proper metric.

The hierarchical error estimates are based on enrichment of the primary finite element space with bubble functions b_k [12]. The basic idea of these estimates is that the discretization error over the triangle Δ may be approximated as follows:

$$\|\nabla e\|_{L^2(\Delta)} \simeq \left\| \sum_{k=1}^{3} \gamma_k \nabla b_k \right\|_{L^2(\Delta)}. \tag{13}$$

The straightforward and the most expensive method for calculating the coefficients γ_k is via solution of a larger finite element problem. If the primary finite element method results in the algebraic problem

$$A_{LL} U_L^* = F_L, \tag{14}$$

the enriched method requires to solve

$$\begin{bmatrix} A_{LL} & A_{LQ} \\ A_{QL} & A_{QQ} \end{bmatrix} \begin{bmatrix} U_L \\ U_Q \end{bmatrix} = \begin{bmatrix} F_L \\ F_Q \end{bmatrix},$$

where subscripts L and Q stand for linear and quadratic terms. If the solution U_L^* of the primary problem is known, the following algebraic problem for the error has to be solved:

$$\begin{bmatrix} A_{LL} & A_{LQ} \\ A_{QL} & A_{QQ} \end{bmatrix} \begin{bmatrix} D_L \\ D_Q \end{bmatrix} = \begin{bmatrix} F_L - A_{LL} U_L^* \\ F_Q - A_{QL} U_L^* \end{bmatrix}. \tag{15}$$

The entries of vector D_Q are the sought coefficients γ_k in (13).

The exact solution of (15) is too expensive. A cheaper calculation of coefficients γ_k is based on the solution $\tilde{D}_Q$ of the reduced algebraic problem:

$$A_{QQ} \tilde{D}_Q = F_Q - A_{QL} U_L^*. \tag{16}$$

Using a local finite element analysis, one can show equivalence of energy norm of errors in both calculations when the mesh is shape-regular [12]. The matrix A_{QQ} is well-conditioned for such meshes; therefore, the vector $\tilde{D}_Q$ can be calculated efficiently with a simple Krylov subspace method. Our numerical experiments show that the equivalence of the energy norms may hold on anisotropic meshes aligned with the solution.

6. Numerical minimization of energy norm of the discretization error

In this section we consider a few boundary value problems ranging from a simple linear isotropic diffusion equation to a nonlinear transonic potential equation. We denote the linear combination of bubble functions with coefficients γ_k defined by entries of vectors D_Q and $\tilde{D}_Q$ as d_h and $\tilde{d}_h$, respectively.

6.1. Linear diffusion problem with isotropic solution

Let Ω be a unit disk with a radial cut. We consider the classical crack problem with the exact solution

$$u(r, \theta) = r^{1/4} \sin\left(\frac{\theta}{4}\right),$$

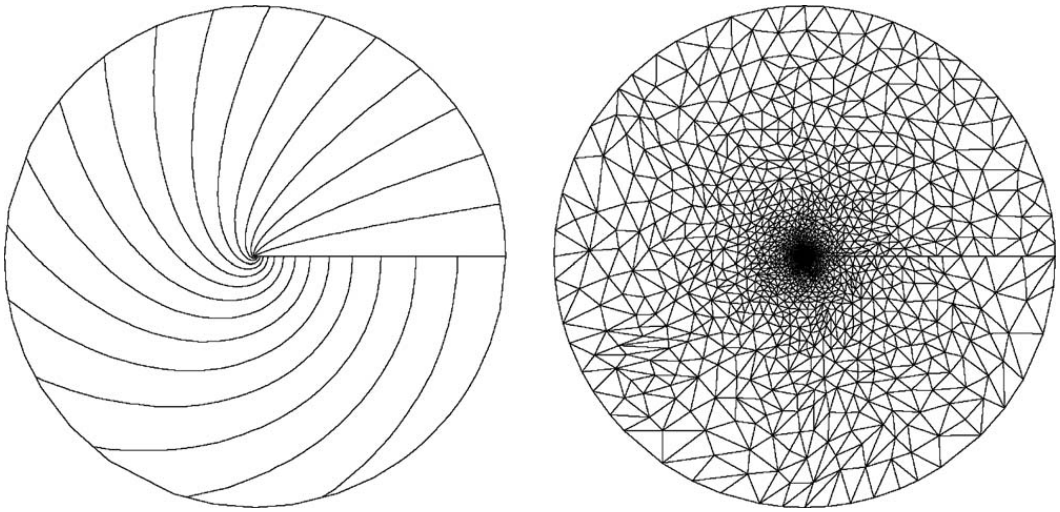

Fig. 2. Solution isolines and the quasi-optimal mesh with roughly 4000 triangles for the crack problem.

where $(r,\ \theta)$ are polar coordinates, $r>0$ and $\theta \in [0,\ 2\pi)$. The crack line S connects points $(0,\ 0)$ and $(1,\ 0)$. We consider the following boundary value problem:

$$\begin{aligned} &\Delta u = 0 \quad \text{in} \quad \Omega \setminus S, \\ &u = \sin\frac{\theta}{4} \quad \text{on} \quad \partial\Omega \setminus S, \\ &u = 0 \quad \text{on} \quad S^+, \quad \frac{\partial u}{\partial n} = 0 \quad \text{on} \quad S^-, \end{aligned} \tag{17}$$

where S^+ and S^- denote the crack line when it is approached from regions $\theta \to +0$ and $\theta \to 2\pi$, respectively.

Fig. 2 shows isolines of the exact solution and the quasi-optimal mesh with roughly 4000 triangles. Most of the triangles are packed around the singularity point $(0,\ 0)$. It takes 8 iterations of Algorithm 1 to reduce the initial discretization error (calculated on a uniform mesh) to a 5% neighborhood of the final error. Solution of problem (14) requires up to 50 iterations whereas solution of reduced problem (16) takes 3 iterations. In both cases we used the Bi-Conjugate Gradient Stabilized (BiCGStab) method with a black-box second-order ILU preconditioner.

The last column in Table 2 demonstrates the half-order convergence of the gradient of the true discretization error for the P_1 finite element approximations. A similar convergence is observed for the gradient of the finite element function $\tilde{d}_h$, which confirms the theory of hierarchical error estimates on shape-regular meshes. The difference in norms of $\tilde{d}_h$ and d_h indicates that the constant of spectral equivalence of energy norms is close to 1.

Table 2
Error estimates and the true discretization error for the crack problem.

N_h	$\|\nabla \tilde{d}_h\|_{L^2(\Omega)}$	$\|\nabla d_h\|_{L^2(\Omega)}$	$\|\nabla e\|_{L^2(\Omega)}$
1000	1.02e−1	1.08e−1	1.09e−1
4000	5.20e−2	5.42e−2	5.38e−2
16,000	2.62e−2	2.72e−2	2.73e−2
64,000	1.30e−2	1.36e−2	1.52e−2
Rate	0.5	0.5	0.47

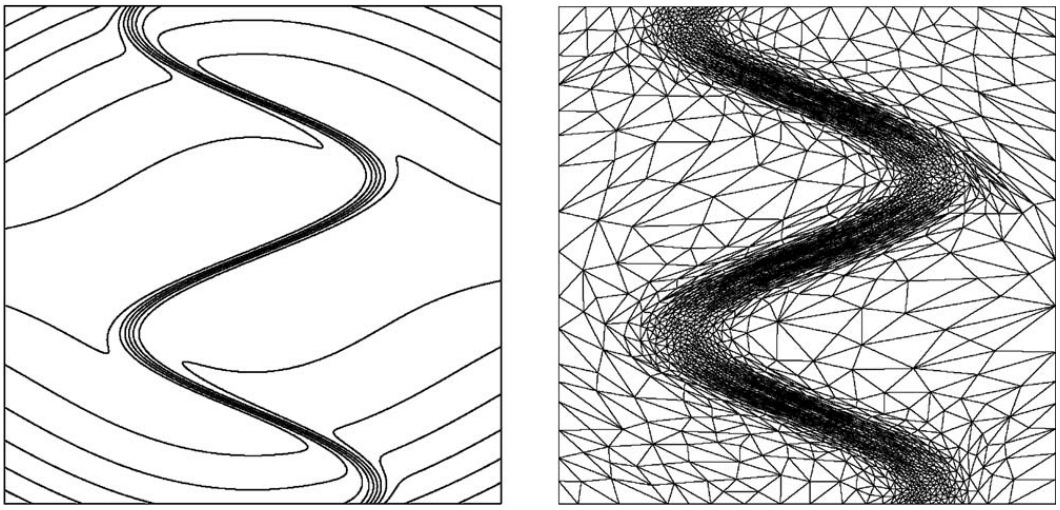

Fig. 3. Solution isolines and the quasi-optimal mesh with roughly 4000 triangles for the anisotropic diffusion problem.

6.2. Linear diffusion problem with anisotropic solution

Let Ω be the unit square $\Omega = (-1, 1)^2$. We consider the following boundary value problem:

$$\begin{aligned} -\mathrm{div}(K\,\nabla u) &= f \quad \text{in } \Omega, \\ u &= u_0 \quad \text{on } \partial\Omega, \end{aligned}$$

where K is the diagonal tensor with entries 1 and 0.1. The right-hand side and the Dirichlet boundary data are such that the exact solution is given by (12).

The quasi-optimal mesh with roughly 4000 triangles is shown in Fig. 3. The maximal ratio of radii of superscribed to inscribed circles is about 7600. The triangles are stretched along the central sine-type curve. It takes only 3–4 iterations of Algorithm 1 to reduce the initial discretization error (calculated on a uniform mesh) to a 5% neighborhood of the final error. Solution of problem (14) requires up to 180 iterations whereas solution of reduced problem (16) takes 5 iterations.

Table 3 shows the optimal error reduction on the sequence of quasi-optimal meshes. The energy norm of the hierarchical *a posteriori* error estimator, $\|K^{1/2}\nabla\tilde{d}_h\|_{L^2(\Omega)}$, is in the excellent agreement with $\|K^{1/2}\nabla d_h\|_{L^2(\Omega)}$, even on anisotropic meshes. Again, both estimates are close to the true energy norm of the discretization error.

6.3. Convection-diffusion problem with analytic solution

Let Ω be the unit square $\Omega = (0, 1)^2$. We consider the following boundary value problem:

$$\begin{aligned} -\mathrm{div}(\nu\,\nabla u - \vec{a}u) &= f \quad \text{in } \Omega, \\ u &= u_0 \quad \text{on } \partial\Omega, \end{aligned}$$

Table 3
Error estimates and the true discretization error for the anisotropic diffusion problem.

N_h	$\|K^{1/2}\nabla\tilde{d}_h\|_{L^2(\Omega)}$	$\|K^{1/2}\nabla d_h\|_{L^2(\Omega)}$	$\|K^{1/2}\nabla e\|_{L^2(\Omega)}$
1000	7.52e−1	8.21e−1	8.03e−1
4000	3.60e−1	4.16e−1	3.77e−1
16,000	1.79e−1	2.07e−1	1.87e−1
64,000	9.12e−2	1.29e−1	9.44e−2
Rate	0.51	0.45	0.51

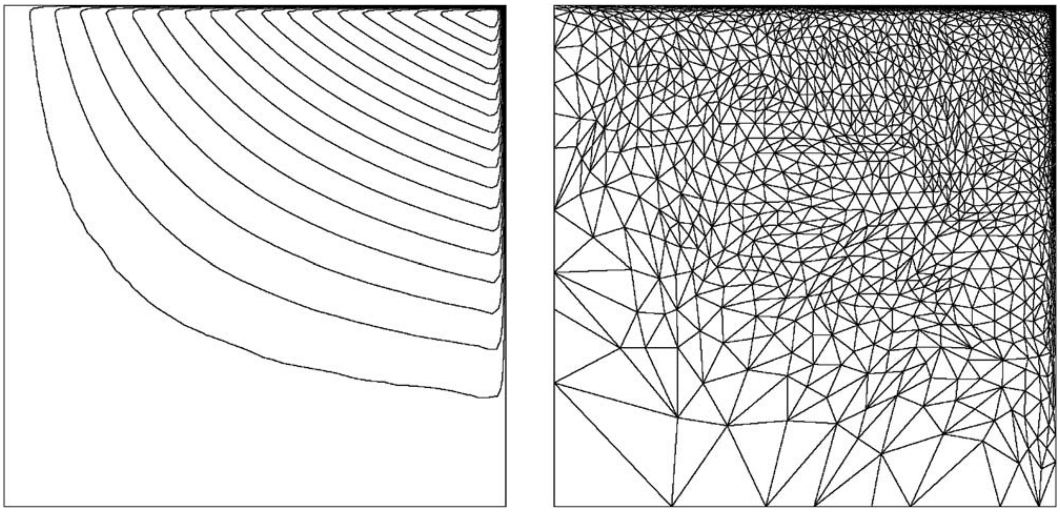

Fig. 4. Solution isolines and the quasi-optimal mesh with roughly 4000 triangles for the convection-diffusion problem.

where $\nu = 10^{-2}$ and $\vec{a} = (2, 3)^T$. The right-hand side and the Dirichlet boundary data are calculated using the exact solution proposed in [20]:

$$u(x,\ y) = \left(x - \exp\left(\frac{2(x-1)}{\nu}\right)\right)\left(y^2 - \exp\left(\frac{3(y-1)}{\nu}\right)\right).$$

The diffusion coefficient ν characterizes thickness of the boundary layer in the top-right corner of Ω.

The quasi-optimal mesh with roughly 4000 triangles is shown in Fig. 4. The maximal ratio of radii of superscribed to inscribed circles reaches 800. It takes 6 iterations of Algorithm 1 to reduce the initial discretization error to a 5% neighborhood of the final error. Solution of problem (14) requires up to 8 iterations whereas solution of reduced problem (16) takes 2 iterations. Note that the SUPG stabilization is *not* used here, since the adaptive mesh itself stabilizes the discretization.

Table 4 shows error reduction on the sequence of quasi-optimal meshes. Deviation from the expected half-order convergence rate is due to slow convergence on coarser meshes. The hierarchical *a posteriori* error estimator is again in the good agreement with the true error.

6.4. Stokes problem

Let Ω be the unit square $(0, 1)^2$. We consider the Stokes problem:

$$\begin{aligned} -\Delta\,\mathbf{u} + \nabla p &= \mathbf{f} \quad \text{in} \quad \Omega, \\ \operatorname{div}\mathbf{u} &= 0 \quad \text{in} \quad \Omega, \\ \mathbf{u} &= 0 \quad \text{on} \quad \partial\Omega \end{aligned} \tag{18}$$

Table 4
Error estimates and the true discretization error for the convection-diffusion problem.

N_h	$\|\nu^{1/2}\nabla\tilde{d}_h\|_{L^2(\Omega)}$	$\|\nu^{1/2}\nabla e\|_{L^2(\Omega)}$
4000	1.73e−1	9.63e−2
16,000	9.53e−2	5.33e−2
64,000	5.16e−2	3.04e−2
256,000	2.70e−2	1.67e−2
Rate	0.45	0.42

Table 5
True discretization errors for $\mathcal{I}_1\mathbf{u}_h$ and $\mathbf{u}_h$ for the Stokes problem.

N_h	$\tilde{E}(\mathbf{u})$	$E(\mathbf{u})$
1000	3.3e−1	2.8e−2
4000	1.6e−1	8.3e−3
16,000	8.1e−2	2.3e−3
64,000	4.0e−2	6.6e−4
Rate	0.5	0.9

with the exact solution $(\mathbf{u}, p)$ [6], where $\mathbf{u} = (v, w)$ and

$$v(x,y) = \left(1 - \cos\left(\frac{2\pi(e^{R_1 x}-1)}{e^{R_1}-1}\right)\right)\sin\left(\frac{2\pi(e^{R_2 y}-1)}{e^{R_2}-1}\right)\frac{R_2}{2\pi}\frac{e^{R_2 y}}{(e^{R_2}-1)},$$

$$w(x,y) = -\sin\left(\frac{2\pi(e^{R_1 x}-1)}{e^{R_1}-1}\right)\left(1 - \cos\left(\frac{2\pi(e^{R_2 y}-1)}{e^{R_2}-1}\right)\right)\frac{R_1}{2\pi}\frac{e^{R_1 x}}{(e^{R_1}-1)},$$

$$p(x,y) = \sin\left(\frac{2\pi(e^{R_1 x}-1)}{e^{R_1}-1}\right)\sin\left(\frac{2\pi(e^{R_2 y}-1)}{e^{R_2}-1}\right)R_1 R_2\frac{e^{R_1 x}e^{R_2 y}}{(e^{R_1 x}-1)(e^{R_2 y}-1)}.$$

We set $R_1 = 4.2985$ and $R_2 = 0.1$ and calculate the right-hand fide $\mathbf{f}$ by substituting the exact solution in (18). The velocity field $\mathbf{u}$ represents a counterclockwise vortex whose center has coordinates

$$x_0 = \frac{1}{R_1}\log\left(\frac{e^{R_1}+1}{2}\right), \qquad y_0 = \frac{1}{R_2}\log\left(\frac{e^{R_2}+1}{2}\right).$$

Higher values of R_1 and R_2 make the center (x_0, y_0) to approach the right-top corner of Ω. The appropriate choice of R_1 and R_2 allows us to mimic boundary layers.

The stable Hood–Taylor $P_2 - P_1$ pair of finite element spaces for $\mathbf{u}$ and p is used for discretization of problem (18). The finite element solution $\mathbf{u}_h$ is known to minimize the energy norm of velocity components:

$$E(\mathbf{u}) = \left(\|\nabla(v_h - v)\|^2_{L^2(\Omega)} + \|\nabla(w_h - w)\|^2_{L^2(\Omega)}\right)^{1/2}.$$

On quasi-uniform meshes this property guarantees $O(h)$ reduction of $E(\mathbf{u})$ for $\mathbf{u} \in (H^2(\Omega))^2$ and $O(h^2)$ reduction of $E(\mathbf{u})$ for $\mathbf{u} \in (H^3(\Omega))^2$. For other meshes with N_h triangles, the optimal convergence rate is the half-order, $N_h^{-1/2}$, for $\mathbf{u} \in (H^2(\Omega))^2$, and the first-order, N_h^{-1}, for $\mathbf{u} \in (H^3(\Omega))^2$.

We note that our approach provides the optimal rate of gradient error reduction for P_1 finite element solution rather than for P_2 finite element solution. We suggest to minimize the gradient error of the P_1 counterpart $\mathcal{I}_1\mathbf{u}_h = (\mathcal{I}_1 v_h, \mathcal{I}_1 w_h)$ of the P_2 velocity $\mathbf{u}_h = (v_h, w_h)$. To generalize our method to vector functions, we define two sets of key values γ_k avoiding the solution of system (16):

$$\gamma_k^{(1)} = (v_h - \mathcal{I}_1 v_h)(\mathbf{c}_k) \qquad \text{and} \qquad \gamma_k^{(2)} = (w_h - \mathcal{I}_1 w_h)(\mathbf{c}_k)$$

and set

$$\alpha_k = (|\gamma_k^{(1)}| + |\gamma_k^{(2)}|)\ ((\mathbb{B}\boldsymbol{\gamma}^{(1)},\ \boldsymbol{\gamma}^{(1)}) + (\mathbb{B}\boldsymbol{\gamma}^{(2)},\ \boldsymbol{\gamma}^{(2)}))\left(\sum_{k=1}^{3}|\gamma_k^{(1)}| + |\gamma_k^{(2)}|\right)^{-1}.$$

It is possible to prove that the sequence of quasi-optimal meshes yields the half-order convergence of the error

$$\tilde{E}(\mathbf{u}) = \left(\|\nabla(\mathcal{I}_1 v_h - v)\|^2_{L^2(\Omega)} + \|\nabla(\mathcal{I}_1 w_h - w)\|^2_{L^2(\Omega)}\right)^{1/2}$$

on anisotropic meshes. The linear interpolant in $\tilde{E}(\mathbf{u})$ prevents us from proving a better estimate.

The velocity streamlines and the quasi-optimal mesh with approximately 1000 triangles are shown in Fig. 5. It takes 3 iterations of Algorithm 1 to reduce the initial discretization error to a 5% neighborhood of the final error. In Table 5

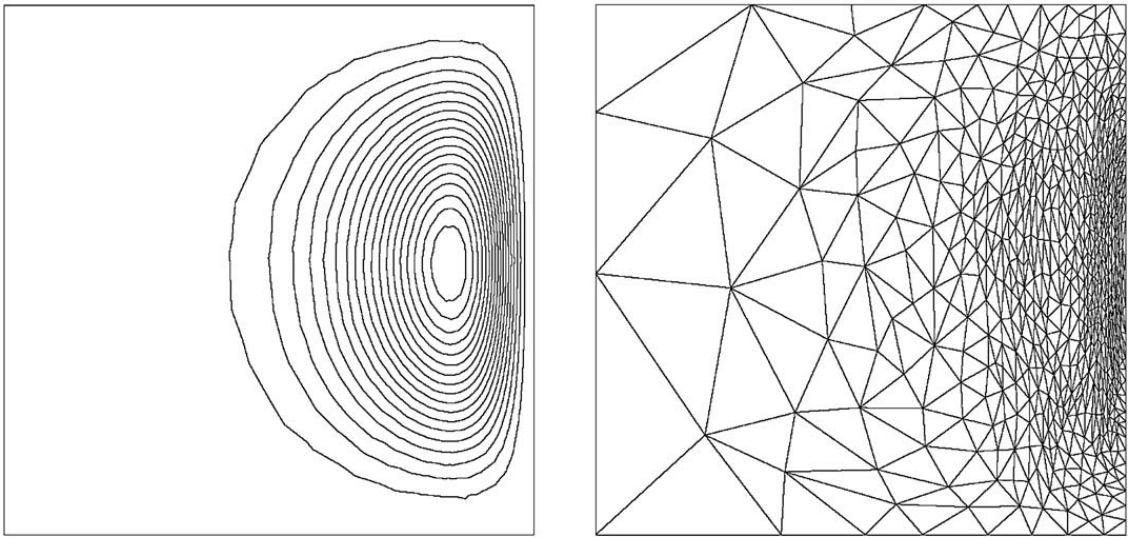

Fig. 5. Velocity streamlines and the adaptive mesh with roughly 1000 triangles for the Stokes problem.

we present the errors $\tilde{E}(\mathbf{u})$ and $E(\mathbf{u})$ on a sequence of adaptive meshes. Optimal half-order convergence rate is observed for $\tilde{E}(\mathbf{u})$. Surprisingly, these meshes provide almost the first-order convergence rate for error $E(\mathbf{u})$.

6.5. Steady-state Navier–Stokes equations

Let Ω be the unit square $(0, 1)^2$. We consider the Navier–Stokes equations

$$\begin{aligned} -0.1\Delta\,\mathbf{u} + (\mathbf{u}\cdot\nabla)\mathbf{u} + \nabla p &= \mathbf{f} \quad \text{in} \quad \Omega, \\ \operatorname{div}\mathbf{u} &= 0 \quad \text{in} \quad \Omega, \\ \mathbf{u} &= 0 \quad \text{on} \quad \partial\Omega \end{aligned} \tag{19}$$

with the analytic solution $(\mathbf{u}, p)$ used for the Stokes problem. The stable Hood–Taylor pair of finite element spaces is used to solve the problem. We use inexact Newton–Krylov solver and the direct solver from the library UMFPACK for linearized problems. The average number of Newton iterations is 4.

Table 6 demonstrates the optimal half-order convergence rate of error $\tilde{E}(\mathbf{u})$ and almost the first-order convergence rate for error $E(\mathbf{u})$.

Table 6
True discretization errors for $\mathcal{I}_1\mathbf{u}_h$ and $\mathbf{u}_h$ for the Navier–Stokes problem.

N_h	$\tilde{E}(\mathbf{u})$	$E(\mathbf{u})$
1000	3.3e−1	7.2e−2
4000	1.6e−1	2.1e−2
16,000	8.1e−2	6.1e−3
64,000	4.0e−2	1.7e−3
Rate	0.5	0.9

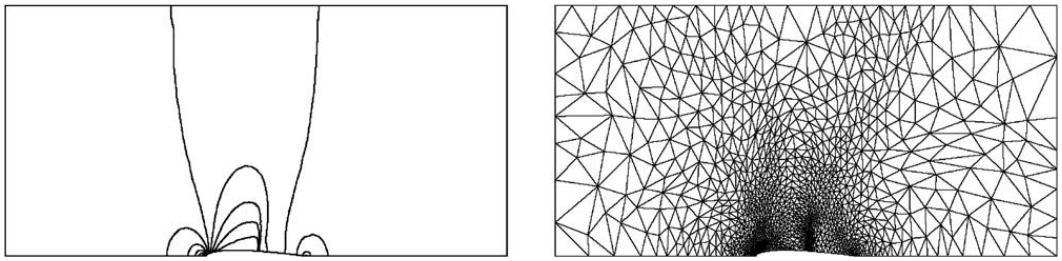

Fig. 6. Isolines of the velocity module and the adaptive mesh with roughly 2000 triangles.

Table 7
Convergence of the hierarchical *a posteriori* error estimator the transonic potential flow problem.

N_h	$\|K^{1/2}\nabla\tilde{d}_h\|_{L^2(\Omega)}$
500	0.18
1000	0.12
2000	0.090
4000	0.065
Rate	0.49

6.6. Transonic potential flow problem

We consider the stationary irrotational adiabatic flow of the ideal gas around a wing-shaped obstacle. The obstacle is the top half of the NACA0012 profile scaled to the segment $[0.4,\ 0.6]$. The computational domain is the rectangle $(0,\ 1)\times(0,\ 0.5)$ without the obstacle. The velocity potential φ satisfies the following equation:

$$\begin{aligned} &\operatorname{div}\left[\left(1-\frac{|\nabla\varphi|^2}{c}\right)^{\alpha}\nabla\varphi\right]=0 \quad \text{in} \quad \Omega,\\ &\frac{\partial\varphi}{\partial n}=\mathbf{u}_\infty\cdot\mathbf{n} \qquad\qquad\quad \text{on} \quad \Gamma_\infty,\\ &\frac{\partial\varphi}{\partial n}=0 \qquad\qquad\qquad\quad \text{on} \quad \Gamma_{bot}. \end{aligned} \tag{20}$$

Here $\mathbf{u}_\infty$ is the flow speed at infinity which is transformed into the Neumann boundary condition for the velocity potential on Γ_∞. The boundary Γ_∞ consists of three linear pieces of $\partial\Omega$ which are entire sides of the rectangle, and the bottom side $\Gamma_{bot}=\partial\Omega\setminus\bar{\Gamma}_\infty$. Further, $c=2c_0^2/(\gamma-1)$, where c_0 is the speed of sound in the motionless gas, $\alpha=1/(\gamma-1)$ and $\gamma=1.4$. The inflow is parallel to the x-axis and its speed is 0.8 Mach. The details of the finite element solution of this problem can be found in [5].

The flow regime is transonic: a shock is formed on the obstacle boundary behind the supersonic zone. Fig. 6 shows the velocity isolines and the quasi-optimal mesh with approximately 2000 triangles.

The mesh adaptation strategy is similar to that for the diffusion problem with the scalar coefficient $K=(1-(|\nabla\varphi|^2/c))^{\alpha}$. Only one step of Algorithm 1 is performed for problem (20). The analytic solution is unknown. Table 7 shows the half-order convergence rate for the hierarchical a posteriori error estimator $\|K^{1/2}\nabla\tilde{d}_h\|_{L^2(\Omega)}$ on the sequence of adapted meshes.

7. Conclusion

We described the new method for generating meshes that minimize the gradient of the FEM discretization error. We have shown that for a mesh with N triangles, the L^2-norm of gradient of error is proportional to $N^{-1/2}$. Numerous numerical experiments verified robustness of the hierarchical error estimator for anisotropic meshes. Optimal reduction of the discretization error was observed on a sequence of quasi-optimal meshes for a wide spectrum of linear and non-linear boundary value problems.

Acknowledgement

Research of the third author was supported in part by the Russian Foundation for Basic Research through grants 08-01-00159, 09-01-00115, by the RAS program "Optimal methods for problems of mathematical physics", and by the Federal program "Scientific and pedagogical personnel of innovative Russia".

References

[1] A. Agouzal, K. Lipnikov, Yu. Vassilevski, Anisotropic mesh adaptation for solution of finite element problems using hierarchical edge-based error estimates, in: B.W. Clark (Ed.), Proceedings of 18th International Meshing Roundtable, Springer, 2009, pp. 595–610.
[2] A. Agouzal, K. Lipnikov, Yu. Vassilevski, Hessian-free metric-based mesh adaptation via geometry of interpolation error, Comput. Math. Math. Phys. 50 (2010) 124–138.
[3] A. Agouzal, K. Lipnikov, Yu. Vassilevski, Edge-based a posteriori error estimators for generating quasi-optimal simplicial meshes, Math. Model. Nat. Phenom. 5 (2010) 91–96.
[4] A. Agouzal, Yu. Vassilevski, Minimization of gradient errors of piecewise linear interpolation on simplicial meshes, Comput. Methods Appl. Mech. Eng. 199 (2010) 2195–2203.
[5] H. Berger, G. Warnecke, W. Wendland, Finite elements for transonic potential flows, Numer. Methods PDEs 6 (1990) 17–42.
[6] S. Berrone, Adaptive discretization of stationary and incompressible Navier–Stokes equations by stabilized finite element methods, Comput. Methods Appl. Mech. Eng. 190 (2001) 4435–4455.
[7] G. Buscaglia, E. Dari, Anisotropic mesh optimization and its application in adaptivity, Int. J. Numer. Methods Eng. 40 (1997) 4119–4136.
[8] M. Castro-Diaz, F. Hecht, B. Mohammadi, O. Pironneau, Anisotropic unstructured mesh adaptation for flow simulations, Int. J. Numer. Methods Fluids 25 (1997) 475–491.
[9] T. Coupez, A mesh improvement method for 3d automatic remeshing, in: N.P. Weatherill, et al. (Eds.), Numerical Grid Generation in Computational Fluid Dynamics and Related Fields, Pineridge Press, 1994, pp. 615–626.
[10] T. Coupez, Parallel adaptive remeshing in 3d moving mesh finite element, in: B.K. Soni, et al. (Eds.), Numerical Grid Generation in Computational Field Simulations, vol. 1, Mississipi State University, 1996, pp. 783–792.
[11] E. D'Azevedo, Optimal triangular mesh generation by coordinate transformation, SIAM J. Sci. Stat. Comput. 12 (1991) 755–786.
[12] P. Deuflhard, P. Leinen, H. Yserentant, Concepts of an adaptive hierarchical finite element code, IMPACT 1 (1989) 3–35.
[13] L. Formaggia, S. Perotto, Anisotropic error estimates for elliptic problems, Numer. Math. 94 (2003) 67–92.
[14] F. Hecht, A few snags in mesh adaptation loops, in: B.W. Hanks (Ed.), Proceedings of 14th International Meshing Roundtable, Springer-Verlag, 2005, pp. 301–312.
[15] W. Huang, Metric tensors for anisotropic mesh generation, J. Comput. Phys. 204 (2005) 633–665.
[16] W. Huang, Mathematical principles of anisotrpic mesh adaptation, Commun. Comput. Phys. 1 (2006) 276–310.
[17] G. Kunert, An a posteriori residual error estimator for the finite element method anisotropic tetrahedral meshes, Numer. Math. 86 (2000) 471–490.
[18] G. Kunert, A posteriori error estimation for anisotropic tetrahedral and triangular finite element meshes, Ph.D. Thesis, TU Chemnitz, 1999.
[19] K. Lipnikov, Yu. Vassilevski, Parallel adaptive solution of 3D boundary value problems by Hessian recovery, Comput. Methods Appl. Mech. Eng. 192 (2003) 1495–1513.
[20] G. Manzini, A. Russo, A finite volume method for advection-diffusion problems in convection-dominated regimes, Comput. Methods Appl. Mech. Eng. 197 (13–16) (2008) 1242–1261.
[21] Yu. Vassilevski, K. Lipnikov, Adaptive algorithm for generation of quasi-optimal meshes, Comput. Math. Math. Phys. 39 (1999) 1532–1551.
[22] Yu. Vassilevski, A. Agouzal, Unified asymptotic analysis of interpolation errors for optimal meshes, Doklady Math. 72 (2005) 879–882.
[23] R. Verfurth, A Review of a Posteriori Error Estimation and Adaptive Mesh-refinement Techniques, Wiley-Teubner, Stuttgart, Germany, 1996.